ROS

RESEARCH ARTICLES

Increase of Reactive Oxygen Species Associates with the Achievement of Meiotic Competency in Rat Oocytes Cultured In Vitro

Meenakshi Tiwari and Shail K. Chaube

Cell Physiology Laboratory, Biochemistry Unit, Department of Zoology, Institute of Science, Banaras Hindu University, Varanasi-221005, U.P., India

Correspondence: shailchaubey@gmail.com (S.K.C.) or shailchaube@bhu.ac.in (S.K.C.)

Tiwari M and Chaube SK. Reactive Oxygen Species 4(11):320–335, 2017; ©2017 Cell Med Press
http://dx.doi.org/10.20455/ros.2017.853
(Received: July 4, 2017; Accepted: July 9, 2017)

ABSTRACT | Reactive oxygen species (ROS) play an important role during meiotic maturation and ovulation. The downstream impact of ROS during the achievement of meiotic competency remains ill understood. The present study was aimed to find out the impact of ROS on the level of cyclic nucleotides and maturation promoting factor (MPF) during the achievement of meiotic competency. For this purpose, cumulus oocyte complexes (COCs) were collected from the ovary of experimental rats injected with 20 IU pregnant mare's serum gonadotropin (PMSG) for 48 h, and PMSG was followed by 20 IU human chorionic gonadotropin (hCG) for 14 h. The morphological changes, meiotic status of oocyte, brilliant cresyl blue (BCB) staining for meiotic competency, total ROS, hydrogen peroxide (H_2O_2), adenosine 3′,5′-cyclic monophosphate (cAMP), guanosine 3′,5′-cyclic monophosphate (cGMP), cell division cycle 25B (Cdc25B), Wee1, specific phosphorylation status of cyclin-dependent kinase 1 (Cdk1), and cyclin B1 expression levels were analyzed. Data suggest that the culture of diplotene-arrested COCs in vitro resulted in spontaneous as well as hCG-induced meiotic exit from diplotene arrest (EDA) in a time-dependent manner, but the first polar body (PB-I) was not extruded. However, 20 IU hCG surge induced extrusion of PB-I in majority of ovulated oocytes. A moderate increase of total ROS as well as H_2O_2 levels associate with EDA. The cAMP, cGMP, Cdc25B, Thr161 phosphorylated Cdk1 as well as cyclin B1 levels were decreased, while Wee1 and Thr14/Tyr15 phosphorylated Cdk1 levels were significantly increased leading to MPF destabilization. The destabilized MPF resulted in spontaneous EDA in rat COCs cultured in vitro. Taken together, these data suggest that a moderate increase of ROS decreases the cyclic nucleotides level that destabilizes MPF. The destabilized MPF results in EDA in rat COCs cultured in vitro.

KEYWORDS | Cyclic nucleotides; Maturation promoting factor; Meiotic exit; Rat cumulus oocyte complexes; Oocytes; Reactive oxygen species

ABBREVIATIONS | ART, assisted reproductive technology; BCB, brilliant cresyl blue; Cdc25B, cell division cycle 25B; COCs, cumulus oocyte complexes; CTCF, corrected total cell fluorescence; FITC,

fluorescein isothiocyanate; GV, germinal vesicle; GVBD, germinal vesicle breakdown; H_2DCFDA, 2′,7′-dichlorodihydrofluorescein diacetate; hCG, human chorionic gonadotropin; LH, luteinizing hormone; M-I, metaphase-I; M-II, metaphase-II; PB-I, first polar body; PMSG, pregnant mare's serum gonadotropin; ROS, reactive oxygen species; TRITC, tetra methyl rhodamine isothiocyanate

CONTENTS

1. INTRODUCTION

Meiotic cell cycle in mammalian oocyte is a long and protracted process that involves several stop/go channels [1–3]. Oocytes are physiologically arrested at the diplotene stage within ovarian follicles from birth to puberty in mammals [4–7]. These diplotene-arrested oocytes, so called as dictyate stage oocytes, are morphologically identified by the presence of germinal vesicle (GV) in the cytoplasm and nucleolus within the GV [5, 8]. The cell cycle arrest for such a long period is due to continuous transfer of several signal molecules and inhibitory factors via gap junctions from encircling granulosa cells to the oocyte inside the follicular microenvironment [2, 4, 7, 8]. Pituitary gonadotropins surge disrupts gap junctions and thereby cumulus-oocyte communications ensuing interruption in supply of inhibitory factors to the oocyte leading to meiotic exit from diplotene arrest (EDA) [1, 9, 10]. Furthermore, the physical removal of encircling granulosa cells also disrupts the supply of inhibitory factors from granulosa cells to the oocyte causing spontaneous EDA under in vitro culture conditions [11–18].

Studies suggest that the growing oocytes encompass higher glucose-6-phosphate dehydrogenase (G6PDH) activity as compared to fully grown oocytes [19]. The nicotinamide adenine dinucleotide phosphate (NADPH) generated by G6PDH can reduce brilliant cresyl blue (BCB) stain, a phenoxazine compound and transform it to a colourless compound (leuco-phenoxazine) [20]. Thus, oocytes that have completed their growth phase show decreased G6PDH and exhibit cytoplasm with blue coloration (BCB^+), whereas growing oocytes, which are expected to have a high level of active G6PDH, remain

colorless (BCB^-) after staining [21]. Therefore, BCB staining has been widely used to select competent oocytes in mouse [19, 22], sheep [23], goat [24], and cattle [25]. Studies have revealed that the embryos derived from (BCB^+) cumulus–oocyte complexes (COCs) had higher developmental competency than embryos derived from (BCB^-) COCs [26–29].

Achievement of meiotic competency starts when oocyte progresses from the diplotene stage to metaphase-I (M-I) stage [4, 10, 13, 17] and further gets physiologically arrested at metaphase-II (M-II) stage by extruding first polar body (PB-I) at the time of ovulation in most of the mammalian species [30–36]. These oocytes remain arrested at the M-II stage even after ovulation until fertilization [2, 14–16, 30–36].

The induction of meiotic maturation and ovulation is achieved by giving human chorionic gonadotropin (hCG) surge in various mammalian species during assisted reproductive technology (ART) programs [37]. Due to structural and biological similarities to luteinizing hormone (LH), hCG binds to LH receptors [37] and induces reactive oxygen species (ROS) generation due to increased cell proliferation during the final stages of folliculogenesis [5, 38]. Another source of ROS could be the inflammation generated due to follicular rupture during ovarian stimulation protocol. This notion is supported by the observations that depletion of ROS level impairs ovulation [38, 39]. The increased level of ROS is beneficial for oocyte meiotic resumption, fertilization, and improved reproductive outcome in human [5, 40].

Several signal molecules and their crosstalk are important during modulation of oocyte physiology in mammals [41]. These signal molecules are generated either by encircling granulosa cells or by oocyte itself [9, 15–17]. Different levels of these signal molecules may decide whether the meiotic cell cycle has to be maintained at the diplotene stage or resumed inside the follicular microenvironment [7, 12–14]. Hydrogen peroxide (H_2O_2), adenosine 3′,5′-cyclic monophosphate (cAMP), and guanosine 3′,5′-cyclic monophosphate (cGMP) are major signal molecules required for modulation of meiotic cell cycle in mammalian oocytes [5, 15–17]. Oscillation of these signal molecules could modulate cell division cycle 25B (Cdc25B), Wee1, maturation promoting factor (MPF) stabilization/destabilization, and/or cyclin-dependent kinase 1 (Cdk1) activity that finally regulate meiotic cell cycle in oocytes [2, 14–17, 31–35, 41, 42].

ROS are commonly generated due to increased cellular metabolism during ovarian stimulation protocol in various ART programs. However, the impact of ROS on other signal molecules and MPF stabilization/destabilization remains poorly understood. Therefore, the present study was aimed to analyze the changes in ROS, H2O2, cAMP, cGMP, Cdc25B, Wee1, and specific phosphorylation status of Cdk1 and cyclin B1 levels during spontaneous EDA to find out possible mechanism of ROS action to destabilize MPF level during the achievement of meiotic competency in rat COCs cultured in vitro.

2. MATERIAL AND METHODS

2.1. Chemicals and Preparation of Culture Medium

The culture media used in the present study were purchased from HiMedia Laboratories (Mumbai, India). All other chemicals were purchased from Sigma Chemical Co. (St. Louis, MO, USA) unless otherwise specified. Culture medium (AL094A, M-199) was prepared as per the manufacture's manual protocol. The sodium bicarbonate (0.035% w/v) was added and the pH was adjusted to 7.2 ± 0.05. The osmolarity was checked (290 ± 5 mOsmol). The culture medium-199 (M-199) was then supplemented with glutamine, penicillin and streptomycin (GPS; 1 µl/ml; Cat. No. A007, HiMedia) to prevent microbial growth and then stored at 4ºC until use (discarded if not used within 15 days). Plain M-199 was used for handling COCs and washing purpose, while 5% fetal bovine serum (FBS) was added to M-199 and then used for in vitro studies.

2.2. Collection of COCs

The immature female rats (Rattus norvegicus) of Charles-Foster strain (22–24 days old; 45±5 g body weight) were housed in a light-controlled room with food and water ad libitum. In the first series of experiments, rats were subjected to a single subcutaneous injection of 20 IU pregnant mare's serum gonadotropin (PMSG) for 48 h and then the experimental rats were euthanized. The ovary along with fallopian tube was collected in pre-warmed M-199. The ovary was punctured using a 26-gauge needle attached to a 1 ml of tuberculin syringe under a microscope (Nikon

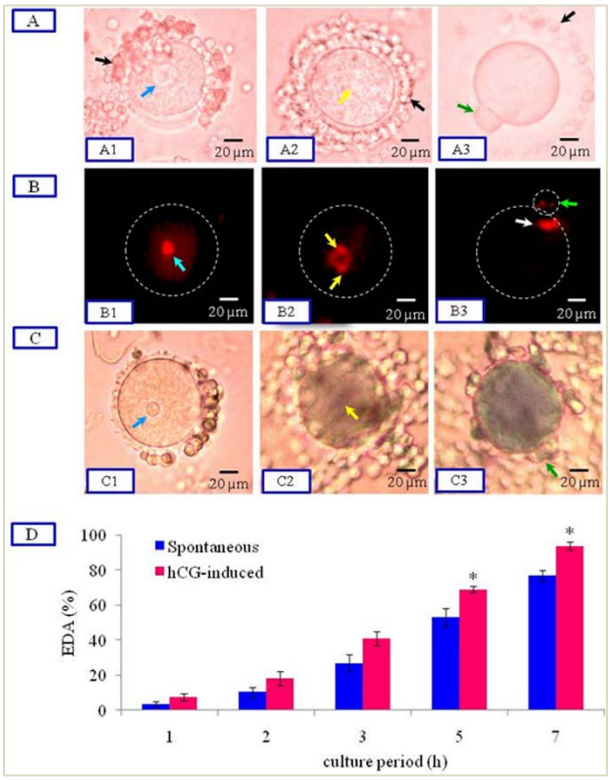

FIGURE 1. Representative photographs showing morphological changes in COCs. COCs collected from PMSG-treated rats showed diplotene arrest as evidenced by the presence of GV and nucleolus in COCs (Blue arrow, A1). These oocytes were tightly encircled with several layers of granulosa cells (black arrow, A1). The spontaneous and hCG-induced EDA in COCs were evidenced by germinal vesicle breakdown (GVBD) and absence of nucleolus (yellow arrow, A2). Ovulated COCs showed maintenance of M-II stage, PB-I extrusion (green arrow, A3) and cumulus cell dispersion (black arrow, A3) after 14 h of hCG surge. The diploid set of chromosomes confirmed the diplotene arrest (Blue arrow, B1), while formation of metaphase plate (yellow arrows) indicated spontaneous as well as hCG-induced EDA (B2). M-II arrest was confirmed by haploid set of chromosomes in oocyte cytoplasm (white arrow, B3) and another set of chromosomes in PB-I (green arrow, B3). The diplotene-arrested COCs showing BCB^{-} staining as the COCs did not take any stain (C1). COCs that showed EDA exhibited BCB^{+} stain as evidenced by faint blue coloured cytoplasm (C2). M-II arrested COCs showed BCB^{+} stain as evidenced by blue coloured cytoplasm (C3). Culture of diplotene-arrested COCs with or without 2 IU hCG induced EDA in a time-dependent manner. Data are mean ± SEM of three independent experiments and analyzed by two-way ANOVA followed by Bonferroni post-hoc analysis. The Bonferroni post-hoc analysis suggested that the rate of hCG induced EDA was higher than that of spontaneous EDA, *$p < 0.05$. Bar = 20 µm.

type 104, Japan) in 35 mm Petri dish containing 2 ml of pre-warmed M-199. The diplotene-arrested COCs were collected using microtubing attached with a disposable glass micropipette (Clay-Adams, NJ, USA). The diplotene-arrested COCs were identified morphologically by the presence of GV and nucleolus in oocyte cytoplasm.

To induce spontaneous EDA, diplotene-arrested COCs were cultured for 7 h in vitro. The EDA was also induced by exposing diplotene-arrested COCs to 2 IU hCG. The diplotene-arrested COCs (18–20 COCs in each group) were cultured with or without hCG for 1, 2, 3, 5, and 7 h in a CO2 incubator (Galaxy 170R, New Brunswick, Eppendorf AG, Hamburg, Germany; 37ºC, 5% CO_2, and 100% humidity). Absence of GV was treated as EDA and used for further analysis in the present study.

For the collection of M-II-arrested COCs, rats were subjected to a superovulation induction protocol (20 IU PMSG for 48 h followed by 20 IU hCG for 14 h). The ovulated COCs (36–40 COCs/animal) were collected from the ampulla of fallopian tube and further cultured for 15 min in M-199 to induce the release of PB-I. The presence of PB-I with normal morphology was treated as M-II arrested COCs in the present study.

Some of the COCs from each group were transferred to M-199 containing 0.01% hyaluronidase at 37ºC and denuded by repeated manual pipetting. Approximately 12–14 COCs and denuded oocytes (6–8) from each group were washed three times with plain M-199 and then analyzed for morphological changes using a phase-contrast microscope (Nikon, Eclipse; E600, Tokyo, Japan) at 400× magnification. These COCs and denuded oocytes were transferred on a slide and fixed with 4% buffered formaldehyde.

In the second series of experiments, in vitro studies were conducted as described for the first series and approximately 36–40 COCs from all groups were

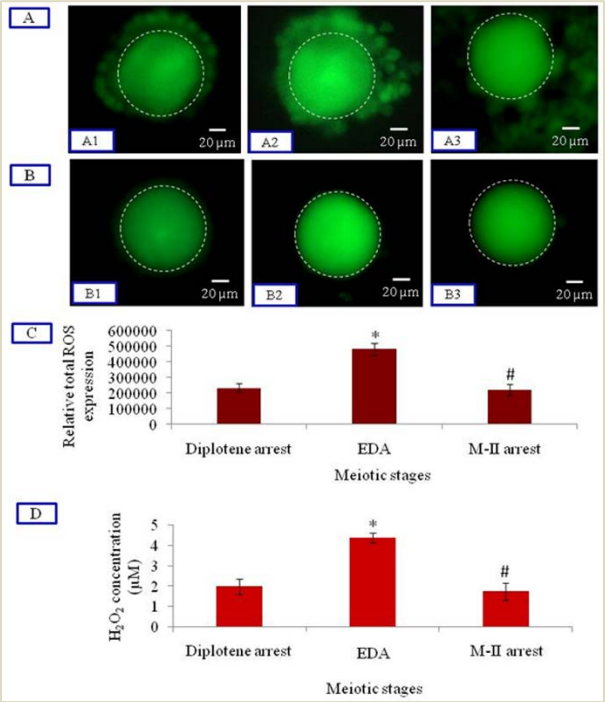

FIGURE 2. Representative photographs showing DCF fluorescence intensity of total ROS level in COCs and H_2O_2 concentration in denuded oocytes. A moderate increase of DCF fluorescence intensity in COCs was observed during spontaneous as well as hCG-induced EDA (A2) as compared to diplotene-arrested COCs (A1). The ROS level decreased in M-II arrested COCs collected after 14 h post-hCG surge (A3). The CTCF analysis of denuded oocytes (B1-3) of corresponding COCs (A1-3) using ImageJ software further confirmed the above observations (C). The spontaneous as well as hCG-mediated EDA were associated with a significant increase of intraoocyte H_2O_2 concentration. The H_2O_2 level was declined in M-II arrested oocytes (D). Data are mean ± SEM of three independent experiments and analyzed by Student's t-test; *$p < 0.001$ (C), $^{\#}p < 0.05$ (D), significantly increased (Diplotene arrest versus EDA); $^{\#}p < 0.001$ (C), $^{\#}p < 0.05$ (D), significantly decreased (EDA versus M-II arrest). Bar = 20 µm.

denuded and immediately used for the quantitative analysis of H_2O_2, cAMP, as well as cGMP levels. Three independent experiments were conducted using 50 experimental animals to get COCs and denuded oocytes sufficient for morphological, biochemical, and immunofluorescence analysis in the present study. All procedures confirmed to the provisions of Institutional Animal Ethical Committee of the university (wide letter no. F.Sc./IAEC/2014-15/0248).

2.3. Determination of Meiotic Status of Oocytes

The COCs were partially denuded by repeated manual pipetting and after washing with M-199, and the meiotic status of oocyte was confirmed using propidium iodide (PI) staining under a fluorescence microscope (Model Ni-U, Nikon Eclipse, Tokyo, Japan). For this purpose, approximately 12–14 oocytes collected from each group were washed twice with phosphate-buffered saline (PBS) and then incubated with PI (1 mg/ml) for 1 min in PBS. Thereafter, denuded oocytes were washed 6–8 times with PBS and then checked for their meiotic status under a fluorescence microscope at 540 nm (400× magnification). Three independent experiments were conducted to confirm the meiotic stage and representative photographs are shown in the Results section.

2.4. Determination of Meiotic Competency Using BCB Staining

A group of COCs (12–14) were incubated with 26 µM of BCB diluted in M-199 for 30 min in a CO_2 incubator following previously published protocol with minor modifications [29]. At the end of incubation period, COCs were washed 3 times with PBS and then examined for BCB binding in oocyte under a phase-contrast microscope.

2.5. Analysis of Total ROS Level

The total ROS level was analyzed using 2′,7′-dichlorodihydrofluorescein diacetate (H_2DCFDA) following our previously published protocol [10]. Briefly, 12–14 COCs from each group were exposed to H2DCFDA (10 µM) for 15 min at 37ºC in a CO_2 incubator. Thereafter, COCs were washed 5 times with pre-warmed PBS and then the DCF fluorescence was analyzed at 485 nm excitation/520 nm emissions using a fluorescence microscope (400× magnification). The corrected total cell fluorescence (CTCF) of 12–14 denuded oocytes of corresponding COCs from three independent experiments was used for analysis using ImageJ software (version 1.44, National Institutes of Health, Bethesda, USA).

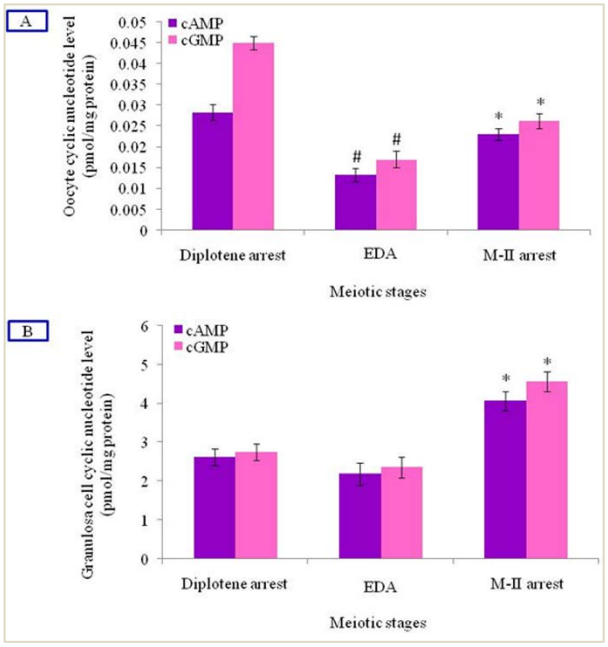

FIGURE 3. Representative histograms showing changes in cyclic nucleotide level in oocytes as well as in granulosa cells. A significant decrease of cAMP and cGMP were observed in denuded oocytes that underwent spontaneous as well as hCG-mediated EDA. Cyclic nucleotide level increased in M-II arrested oocytes after 14 h post-hCG surge (A). Cyclic nucleotide level was higher in encircling granulosa cells of corresponding oocytes. The increased level of both nucleotides in encircling granulosa cells was maintained after 14 h post-hCG surge (B). Data are mean ± SEM of three independent experiments and analyzed by Student's t-test, $^{\#}p < 0.001$, significantly decreased (Diplotene arrest versus EDA); $*p < 0.01$, significantly increased (EDA versus M-II arrest).

2.6. Quantitative Estimation of H_2O_2 Concentration

The H2O2 concentration was analyzed using a hydrogen peroxide assay kit (Cat. No. K265-200) purchased from BioVision (Milpitas, CA, USA. In brief, approximately 36–40 COCs collected from each group were denuded by manual pipetting and lysed in hypotonic lysis buffer (5 mM Tris, 20 mM ethyldiaminetetraacetic acid [EDTA], 0.5% Triton X-100, pH 8.0). Lysates were centrifuged at 10,000 g at 4°C for 30 min and the supernatant was immediately used for quantitative estimation of H2O2 following previously published protocol [13]. The optical density (OD) was determined using a microplate reader (Micro Scan MS5608A, Electronics Corporation of India Limited, Hyderabad, India) set to 550 nm. Samples from three independent experiments were used for each group and all samples were run in one assay to avoid inter-assay variation, and intra-assay variation was 2.3%.

2.7. Quantitative Estimation of cAMP and cGMP Concentrations

The cAMP as well as cGMP concentrations were analyzed using ELISA kits (cAMP: Cat. No. KGE002; cGMP: Cat. No. KGE003) purchased from R&D Systems (Minneapolis MN, USA) as per our previously published protocol [14]. In brief, approximately 36–40 COCs were collected from each group and denuded by manual pipetting. The denuded oocytes and their corresponding granulosa cells were lysed separately in hypotonic lysis buffer (5 mM Tris, 20 mM EDTA, 0.5% TritonX-100, pH 8.0) and centrifuged at 10,000 g at 4°C for 30 min. The supernatant was stored at –20°C until all samples were collected. Reagents, samples, and standards were prepared as per the manufacturer's manual protocol. The OD was taken using a microplate reader set at 450 nm within 10 min. Samples from three independent experiments were run in one assay to avoid inter-assay variation, and intra-assay variation was found to be 1.90%. The cAMP as well as cGMP levels are represented as pmol/mg protein in the Results section.

2.8. Detection of Cdc25B, Wee1, Specific Phosphorylation Status of Cdk1 and Cyclin B1 Expressions

Immunofluorescence of Cdc25B, Wee1, and specific phosphorylation of Cdk1 and cyclin B1 expressions were analyzed in COCs using their highly specific antibodies purchased from Santa Cruz Biotechnology, (Dallas, TX, USA) as per our published protocol with some modifications [36]. In brief, 12–14 COCs from each group were fixed with 4% buffered formaldehyde (10 min) at room temperature. Slides were washed 3 times with pre-warmed PBS and exposed to Triton X-100 (0.01% in PBS) for 10 min at

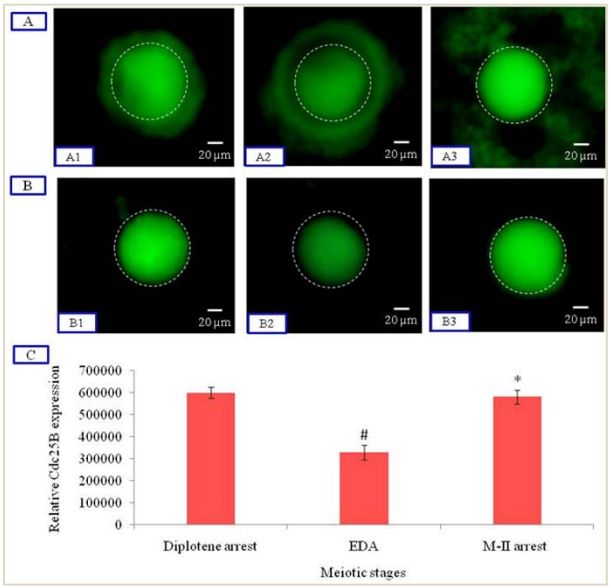

FIGURE 4. Representative photographs showing changes in Cdc25B expression level in COCs. Spontaneous as well as hCG-induced EDA were associated with a significant decrease of Cdc25B expression (A2) as compared to diplotene-arrested COCs (A1). Cdc25B expression was increased in M-II arrested COC_S collected after 14 h post-hCG surge (A3). The CTCF analysis of denuded oocytes (B1-3) of corresponding COCs (A1-3) further confirmed the above observations (C). Data are mean ± SEM of three independent experiments and analyzed by Student's t-test, $^{\#}p < 0.001$, significantly decreased (Diplotene arrest versus EDA); $*p < 0.001$, significantly increased (EDA versus M-II arrest). Bar = 20 µm.

37°C for permeabilization. Slides were washed 3 times with pre-warmed PBS and then treated with sodium citrate solution (0.01 M) at 37°C (10 min). Slides were again washed 3 times with pre-warmed PBS and then incubated with blocking buffer (2.5% PBS-BSA solution) at 37°C (30 min). Thereafter, slides were exposed to 100 µl of their respective primary antibodies (Cdc25B (H-85), rabbit polyclonal antibody (sc-5619) raised against amino acids 93–177 mapping near the N-terminus of Cdc25B; Wee1 (H-300), rabbit polyclonal antibody (sc-9037) raised against amino acids 347–646 mapping at the C-terminus of Wee1; p-Cdc2 p34 (Thr14/Tyr15), rabbit polyclonal antibody (sc-12340) raised against a short amino acid sequence containing Thr14 and Tyr15 phosphorylated Cdc2 p34; p-Cdc2 p34 (Thr161), rabbit polyclonal antibody (sc-12341) raised against a short amino acid sequence containing pThr161 of Cdc2 p-34; Cdc2 p34 (PSTAIRE), rabbit polyclonal antibody (sc-53) raised against a peptide epitope mapping within the conserved PSTAIRE domain of Cdc2 p34; cyclin B1 (H-433), rabbit polyclonal antibody (sc-752) raised against amino acids 1–433 representing full length of cyclin B1; Actin (C-2), mouse monoclonal antibody (sc-8432) specific for an epitope mapping between amino acids 350–375 at the C-terminus of actin; 1:500 dilutions in blocking buffer) at 37°C for 1 h in a CO_2 incubator.

After the above incubation, slides were washed 6–8 times with PBS, and then exposed to 100 µl of specific anti-rabbit fluorescein isothiocyanate (FITC)-labeled (sc-3839) secondary antibody for detection of Cdc25B, Wee1, Thr14/Tyr15, Thr161, as well as total phosphorylated Cdk1 and cyclin B1 levels, and anti-mouse tetramethylrhodamine isothiocyanate (TRITC)-labeled (sc-3796) secondary antibody for detection of β-actin at 37°C in a humidified chamber (1:1000 dilutions in blocking buffer). After 1 h of incubation, slides were washed 5 times with pre-warmed PBS, mounted with fluorescence mounting medium by VECTASHIELD (Vector Laboratories, Burlingame, CA, USA) and then observed under a fluorescence microscope at 465 nm (FITC) and 540 nm (TRITC) at 400× magnification. Fluorescence intensity of β-actin was analyzed in parallel as a control to assure that all parameters were kept constant during immunofluorescence analysis. The experiment was repeated three times and the representative photographs are shown in the Result section.

2.9. Statistical Analyses

Data are expressed as mean ± standard error of mean (SEM) of three independent experiments. All percentage data were subjected to arcsine square root transformation before statistical analysis and then analyzed either by Student's t-test or two-way analysis of variance (ANOVA) followed by Bonferroni post-hoc analysis using the SPSS software, version 17.0 (SPSS Inc., Chicago, IL, USA). A probability of $p < 0.05$ was considered statistically significant.

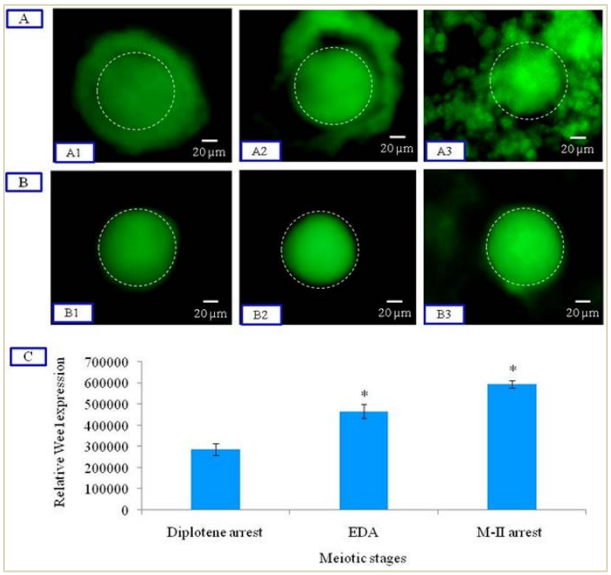

FIGURE 5. Representative photographs showing changes in Wee1 expression level in COCs. A significant increase of Wee1 expression was observed in COCs that underwent spontaneous as well as hCG-induced EDA (A2) as compared to diplotene-arrested COCs (A1). Wee1 expression was further increased in M-II arrested COCs collected after 14 h post-hCG surge (A3). The CTCF analysis of denuded oocytes (B1-3) of corresponding COCs (A1-3) further confirmed our findings (C). Data are mean ± SEM of three independent experiments and analyzed by Student's t-test, *$p < 0.01$, significantly increased (Diplotene arrest versus EDA); *$p < 0.05$, significantly increased (EDA versus M-II arrest). Bar = 20 µm.

3. RESULTS

3.1. Morphological Changes in COCs during In Vitro Culture

As shown in **Figure 1**, COCs collected from PMSG (20 IU for 48 h)-treated animals showed diplotene arrest as evidenced by the presence of GV and nucleolus (blue arrow). These oocytes were encircled with several layers of granulosa cells (black arrow; **Figure 1A1**). COCs showed disappearance of GV and nucleolus (yellow arrow; **Figure 1A2**) during spontaneous as well as hCG (2 IU)-mediated EDA after 7 h of in vitro culture. The majority of oocytes were arrested at M-II stage and possessed PB-I after 14 h of hCG surge (green arrow; **Figure 1A3**). These M-II arrested oocytes showed dispersed encircling granulosa cells (black arrow; **Figure 1A3**). The meiotic stages such as diplotene arrest (**Figure 1B1**), EDA (**Figure 1B2**), and M-II arrest (**Figure 1B3**) were further confirmed by their meiotic status using PI staining.

The BCB test was conducted to determine whether oocytes were meiotically competent or not. Our results show that diplotene-arrested COCs were BCB^- as the COCs did not take any stain (**Figure 1C1**). COCs that showed EDA after 7 h of in vitro culture were meiotically competent as evidenced by BCB^+ faint blue staining (**Figure 1C2**). Furthermore, M-II arrested COCs collected after 14 h hCG surge were also BCB^+ as the oocyte was stained blue (**Figure 1C3**).

As shown in **Figure 1D**, culture of diplotene-arrested COCs in medium with or without 2 IU hCG resulted EDA in a time-dependent manner (two-way ANOVA, spontaneous EDA, $F = 370.49$; hCG-mediated EDA, $F = 336.56$; and interaction between these two factors, $F = 280.42$; $p < 0.001$; **Figure 1D**). Although, hCG induced higher rate of EDA as compared to spontaneous EDA, 2 IU hCG could not induce extrusion of PB-I under in vitro culture conditions. On the other hand, 20 IU hCG surge induced ovulation, extrusion of PB-I, and the majority of oocytes were arrested at M-II stage as evidenced by their chromosomal status (**Figure 1B3**).

3.2. Changes in ROS and H_2O_2 Levels

Figure 2 shows DCF fluorescence intensity of total ROS level in COCs and H_2O_2 concentration in denuded oocytes. A moderate increase of ROS has been observed as evidenced by increase of DCF fluorescence intensity in COCs collected after 7 h of in vitro culture during spontaneous as well as hCG-induced EDA (**Figure 2A2**) compared to diplotene-arrested COCs (**Figure 2A1**). A significant decrease in ROS level was observed in ovulated COCs collected after 14 h post-hCG surge (**Figure 2A3**). The CTCF analysis of denuded oocytes (**Figure 2B1–B3**) of corresponding COCs (**Figure 2A1–A3**) using ImageJ software further confirms our findings (**Figure 2C**). In addition, the spontaneous as well as hCG-mediated EDA were associated with a significant in

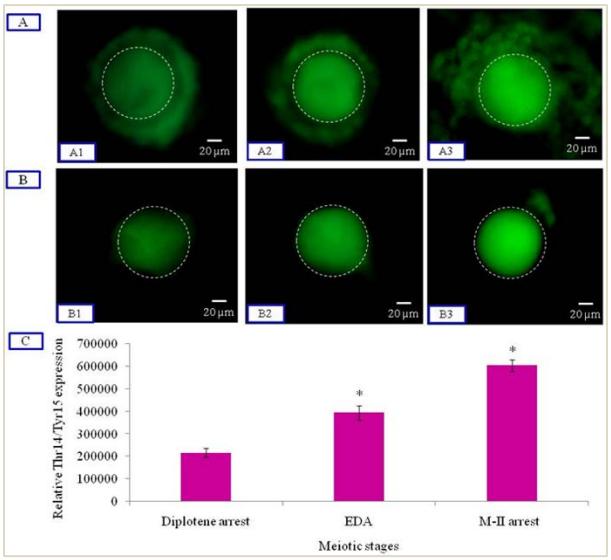

FIGURE 6. Representative photographs showing changes in Thr14/Tyr15 phosphorylated Cdk1 expression level in COCs. A significant increase of Thr14/Tyr15 phosphorylated Cdk1 level was observed in COCs that showed spontaneous as well as hCG-induced EDA (A2) as compared to diplotene-arrested COCs (A1). The Thr14/Tyr15 phosphorylated Cdk1 level was increased in M-II arrested COCs collected after 14 h post-hCG surge (A3). The CTCF analysis of denuded oocytes (B1-3) of corresponding COCs (A1-3) further confirmed our findings (C). Data are mean ± SEM of three independent experiments and analyzed by Student's t-test, *p < 0.01, significantly increased (Diplotene arrest versus EDA); *p < 0.05, significantly increased (EDA versus M-II arrest). Bar = 20 µm.

crease ($p < 0.05$) of intraoocyte H_2O_2 concentration (4.37 ±0.25 µM) as compared to diplotene arrest (1.97 ± 0.38 µM). The H_2O_2 concentration was further declined in M-II arrested oocytes collected after 14 h post-hCG surge (1.73 ± 0.43 µM; **Figure 2D**).

3.3. Changes in Cyclic Nucleotides Level

As shown in **Figure 3**, a significant decrease ($p < 0.001$) of cAMP and cGMP levels was observed in denuded oocytes that underwent spontaneous as well as hCG-mediated EDA as compared to diplotene-arrested denuded oocytes. An increase of cyclic nucleotide levels was observed in M-II arrested oocytes collected after 14 h post-hCG surge (**Figure 3A**). On the other hand, the levels of both cyclic nucleotides were 4–5 times higher in encircling granulosa cells (**Figure 3B**) as compared to the corresponding oocyte (**Figure 3A**). The elevated levels of cAMP and cGMP in encircling granulosa cells were maintained even after 14 h post-hCG surge (**Figure 3B**).

3.4. Changes in Cdc25B Expression Level

As shown in **Figure 4**, a significant decrease ($p < 0.001$) of Cdc25B expression level was observed in COCs that underwent spontaneous as well as hCG-induced EDA (**Figure 4A2**) as compared to diplotene-arrested COCs (**Figure 4A1**). On the other hand, Cdc25B expression was increased in COCs after 14 h post-hCG surge (**Figure 4A3**). The CTCF analysis of denuded oocytes (**Figure 4B1–B3**) of corresponding COCs (**Figure 4A1–A3**) further confirms our findings (**Figure 4C**).

3.5. Changes in Wee1 Expression Level

As shown in **Figure 5**, spontaneous as well as hCG-mediated EDA were associated with a significant increase ($p < 0.01$) of Wee1 expression (**Figure 5A2**) as compared to diplotene-arrested COCs (**Figure 5A1**). Wee1 expression was further increased ($p < 0.05$) in COCs after 14 h post-hCG surge (**Figure 5A3**). The CTCF analysis of denuded oocytes (**Figure 5B1–B3**) of corresponding COCs (**Figure 5A1–A3**) further confirms our results (**Figure 5C**).

3.6. Changes in Thr14/Tyr15 Phosphorylated Cdk1 Expression Level

Figure 6 shows the immunofluorescence intensity of Thr14/Tyr15 phosphorylated Cdk1 level. A significant increase ($p < 0.01$) of Thr14/Tyr15 phosphorylated Cdk1 level was noticed in COCs that underwent spontaneous as well as hCG-induced EDA (**Figure 6A2**) compared to diplotene-arrested COCs (**Figure 6A1**). The level of Thr14/Tyr15 phosphorylated Cdk1 was further increased ($p < 0.05$) in COCs collected after 14 h post-hCG surge (**Figure 6A3**). The CTCF analysis of denuded oocytes (Figure 6B1–B3) of corresponding COCs (**Figure 6A1-A3**) further confirms our observations (**Figure 6C**).

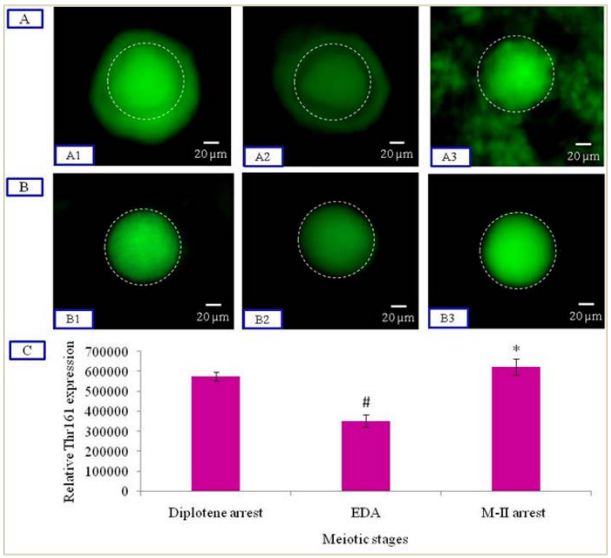

FIGURE 7. Representative photographs showing changes in Thr161 phosphorylated Cdk1 expression level in COCs. Spontaneous as well as hCG-induced EDA were associated with decrease of Thr161 phosphorylated Cdk1 level (A2) as compared to diplotene-arrested COCs (A1). The Thr161 expression was increased in M-II arrested COCs collected after 14 h post-hCG surge (A3). The CTCF analysis of denuded oocytes (B1-3) of corresponding COCs (A1-3) further confirmed our results (C). Data are mean ± SEM of three independent experiments and analyzed by Student's t-test, #p < 0.001, significantly decreased (Diplotene arrest versus EDA); *p < 0.001, significantly increased (EDA versus M-II arrest). Bar = 20 µm.

3.7. Changes in Thr161 Phosphorylated Cdk1 Expression Level

As shown in **Figure 7**, a significant decrease ($p < 0.001$) of Thr161 phosphorylated Cdk1 level was observed in COCs that underwent spontaneous as well as hCG-mediated EDA (**Figure 7A2**) as compared to diplotene-arrested COCs (**Figure 7A1**). On the other hand, Thr161 expression was increased ($p < 0.001$) after 14 h post-hCG surge (**Figure 7A3**). The CTCF analysis of denuded oocytes (**Figure 7B1–B3**) of corresponding COCs (**Figure 7A1–A3**) further confirms our results (**Figure 7C**).

3.8. Total Cdk1 Level Remained Unaltered

As shown in **Figure 8**, total Cdk1 level remained unchanged in the present study. This is evidenced by unaltered immunofluorescence intensity of denuded oocytes (**Figure 8B1–B3**) of corresponding COCs (**Figure 8A1–A3**) of various groups. The CTCF analysis further confirms the above observations (**Figure 8C**).

3.9. Changes in Cyclin B1 Expression Level

As shown in **Figure 9**, spontaneous as well as hCG-induced EDA were associated with a significant decrease ($p < 0.001$) of cyclin B1 expression (**Figure 9A2**) as compared to diplotene-arrested COCs (**Figure 9A1**). On the other hand, cyclin B1 expression was increased ($p < 0.001$) after 14 h post-hCG surge (**Figure 9A3**). The CTCF analysis of denuded oocytes (Figure 9B1–B3) of corresponding COCs (**Figure 9A1–A3**) further confirms our results (**Figure 9C**).

3.10. β-Actin Expression Remained Unchanged

The β-actin expression level was analyzed in parallel as a control for all the immunofluorescence studies carried out in the present study. As shown in **Figure 10**, β-actin expression level did not change in COCs (**Figure 10A1–A3**) and in corresponding denuded oocytes of various groups (**Figure 10B1–B3**). The CTCF analysis of corresponding denuded oocytes further confirms our observations (**Figure 10C**).

4. DISCUSSION

Oocyte quality is one of the important factors that directly affect ARTs outcome in several mammalian species including human [3, 43]. The oocyte quality is solely dependent upon acquisition of meiotic competency, i.e., resumption of meiosis from diplotene arrest, progression via M-I to M-II stage, and release of PB-I that results in the formation of haploid female gamete [3]. The achievement of meiotic competency involves several biochemical and molecular changes [43]. The meiotically competent oocyte determines oocyte quality, and good quality oocytes are required for fertilization and early embryonic development [3, 43].

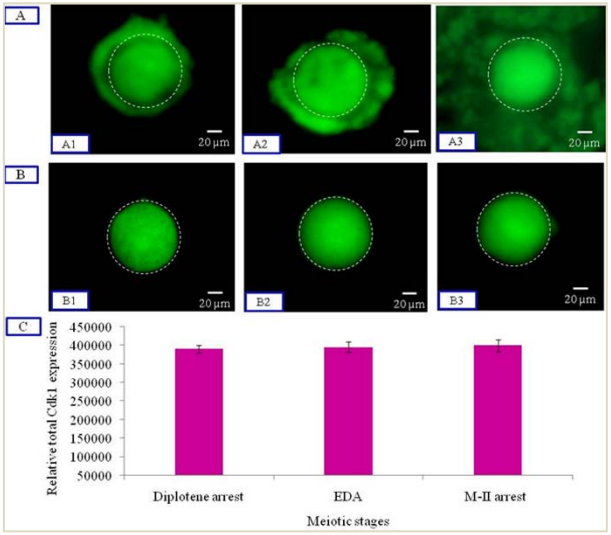

FIGURE 8. Representative photographs showing total Cdk1 level in COCs. The total Cdk1 level remained unaltered. The CTCF analysis of denuded oocytes (B1-3) of corresponding COCs (A1-3) further confirmed the above observations (C). Bar = 20 µm.

Pituitary gonadotropin surge triggers EDA in follicular oocytes, a first step towards the achievement of meiotic competency [10, 37]. Although hCG is commonly used to induce ovulation in several mammalian species [37], its mechanism of action during achievement of meiotic competency remains ill understood. Our data suggest that the majority of oocytes collected after 48 h PMSG surge were arrested at diplotene stage (approximately 95%). Culture of these COCs in vitro resulted in spontaneous EDA in a time-dependent manner. Furthermore, 2 IU hCG induced EDA in a time-dependent manner in vitro. The hCG-induced EDA was always higher than spontaneous EDA. Surprisingly, we could not observe PB-I in COCs that underwent spontaneous as well as hCG (2 IU)-induced EDA under in vitro culture conditions. On the other hand, the superovulation induction protocol induced achievement of meiotic competency as the extrusion of PB-I was observed in more than 95% of oocytes collected from ampulla of fallopian tube and further cultured for 10–15 min in M-199 under in vitro culture conditions. These results suggest that hCG is less effective in inducing EDA under in vitro culture conditions as compared to in vivo surge. The reduced stimulatory effect of hCG under in vitro culture conditions could be due to the removal of the majority of mural granulosa cells encircling oocyte due to physical pressure applied to puncture the follicle at the time of COCs collection in the present study. The encircling mural granulosa cells provide the site of hCG action as they have specific receptors at the level of cell membrane [4, 11, 44].

The meiotic competency of oocytes was further confirmed using BCB staining in the present study. BCB test is an indirect measure of oocyte growth that allows the selection of competent oocytes during in vitro maturation [19]. Data of present study suggest that diplotene-arrested COCs have a high G6PDH activity as the diplotene-arrested COCs did not take any stain (BCB^-). COCs that show EDA after 7 h of in vitro culture have little amount of active G6PDH as evidenced by faint blue BCB stain (BCB^+). However, M-II arrested COCs collected after 14 h hCG surge showed decreased G6PDH and exhibited cytoplasm with blue BCB^+ stain suggesting that these oocytes have achieved meiotic competency. Similarly, BCB staining has been used to select competent oocytes in mouse, sheep, goat, and cattle [22–25].

ROS are commonly generated during ovarian stimulation protocol due to increased cellular metabolism in the ovary. The moderate increase of ROS could be beneficial for oocytes during the achievement of meiotic competency. The generation of ROS mediates spontaneous EDA in oocytes cultured in vitro [7, 13, 45]. Our results suggest that total ROS as well as H_2O_2 levels were significantly increased during spontaneous as well as hCG-induced EDA in vitro. The increased ROS and H_2O_2 levels were associated with the decrease of cAMP as well as cGMP levels during spontaneous as well as hCG-induced EDA. However, the levels of both cyclic nucleotides were increased in M-II arrested oocytes collected after 14 h post-hCG surge. Based on these results, we propose that increase of ROS and decrease of cAMP as well as cGMP levels mediate spontaneous and hCG-induced EDA, while reverse conditions are associated with the maintenance of M-II arrest. Similarly, the increased level of ROS and decreased level of cyclic nucleotides have been reported during spontaneous EDA in rat and human oocytes [10, 13, 14, 44, 46].

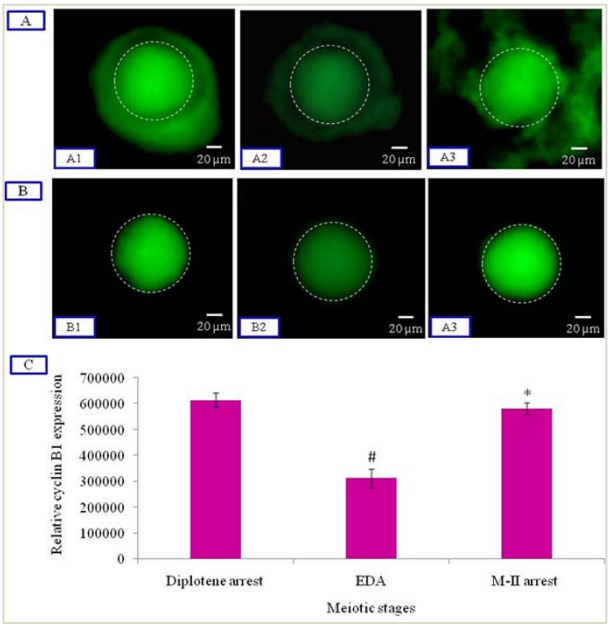

FIGURE 9. Representative photographs showing changes in cyclin B1 expression level in COCs. A decrease of cyclin B1 expression (A2) was observed during spontaneous as well as hCG-induced EDA as compared to diplotene-arrested COCs (A1). The cyclin B1 expression was increased in M-II arrested COCs collected after 14 h post-hCG surge (A3). The CTCF analysis of denuded oocytes (B1-3) of corresponding COCs (A1-3) further confirmed our observations (C). Data are mean ± SEM of three independent experiments and analyzed by Student's t-test, $^{\#}p < 0.001$, significantly decreased (Diplotene arrest versus EDA); $*p < 0.001$, significantly increased (EDA versus M-II arrest). Bar = 20 µm.

The reduction of both cAMP and cGMP levels in oocyte could modulate the downstream pathway to destabilize MPF by altering Cdc25B phosphatase and Wee1 kinase activities. Reduced cGMP level activates cAMP-phosphodiesterase 3A (PDE3A) and reduces the intraoocyte cAMP level [47, 48]. Reduction of intraoocyte cAMP level may result in inactivation of Cdc25B and activation of Wee1 kinase that destabilize MPF leading to meiotic resumption in several mammalian species [4, 49]. This possibility is further supported by the observations that the increased intraoocyte cAMP level activates protein kinase A (PKA), which phosphorylates Cdc25B phosphatase [47, 49]. Data of our present study suggest that Cdc25B expression level was reduced in COCs during spontaneous and hCG-mediated EDA in vitro. On the other hand, Wee1 kinase expression level was increased in a time-dependent manner. These data suggest that inactivation of Cdc25B and activation of Wee1 kinase associate with spontaneous as well as hCG-mediated EDA in the present study.

A moderate increase of ROS level and transient decrease of cyclic nucleotide level can trigger MPF destabilization during spontaneous EDA [10, 13, 46]. Increased ROS level activates Wee1 directly or indirectly and destabilizes MPF by inducing phosphorylation of Thr14/Tyr15 of Cdk1 and cyclin B1 degradation [14, 32, 49]. The destabilized MPF and/or Cdk1 activity trigger EDA in rat oocytes [10, 13, 14]. Data of the present study suggest that Wee1

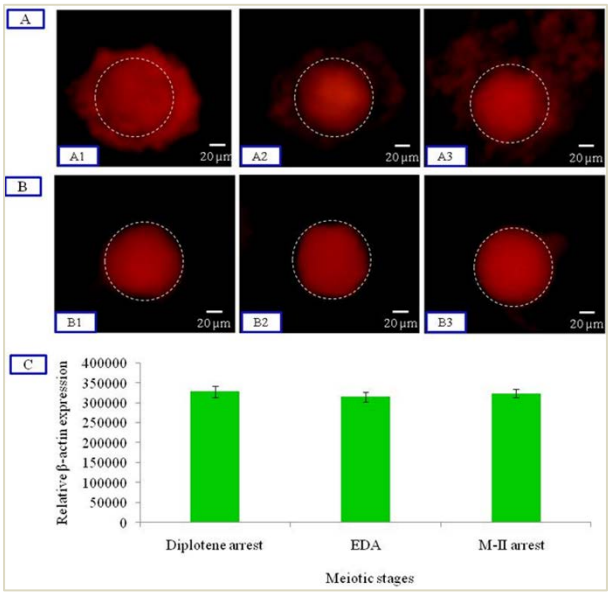

FIGURE 10. Representative photographs showing β-actin expression in COCs. β-Actin expression level did not change in COCs of all groups (A1-3) as well as in their corresponding denuded oocytes (B1-3). The CTCF analysis of corresponding denuded oocytes further confirmed our observations (C).

and Thr14/Tyr15 phosphorylated Cdk1 expression level increased in a time-dependent manner, while

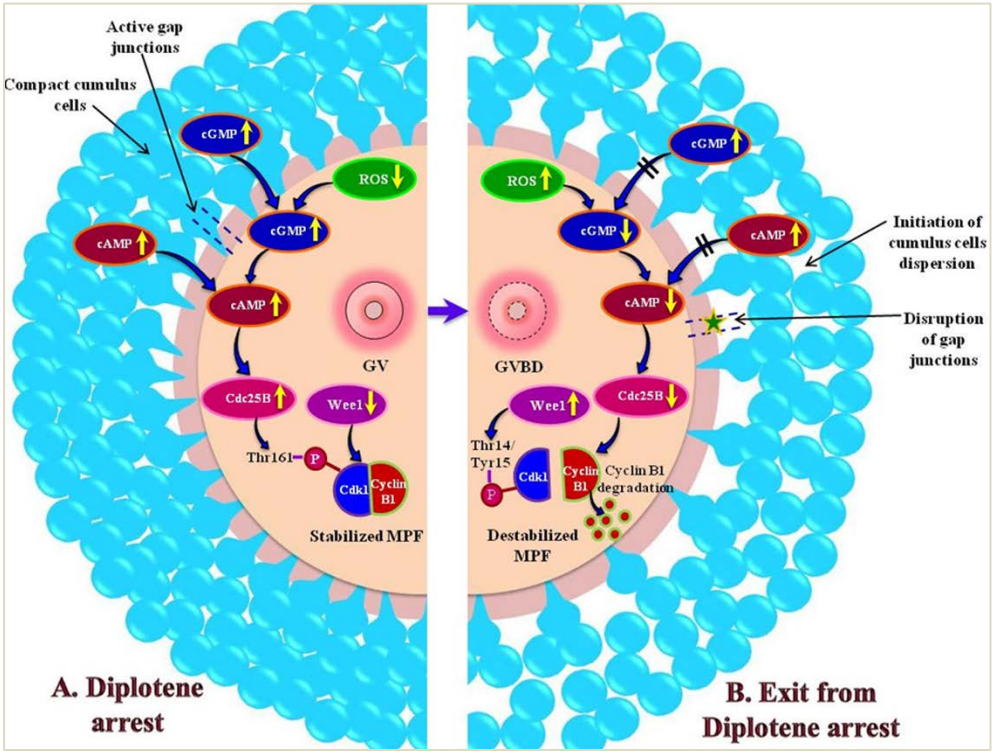

FIGURE 11. A schematic diagram showing a proposed model for the involvement of ROS during EDA in mammalian oocytes. The continuous transfer of cGMP and cAMP via gap junctions elevates the intraoocyte cyclic nucleotide level inside the follicular microenvironment. The increased cAMP level induces Cdc25B phosphatase and Wee1 kinase activities that finally stabilize MPF leading to the maintenance of diplotene arrest (A). The generation of ROS was associated with the decrease of cAMP as well as cGMP levels. The reduced cyclic nucleotide level decreased Cdc25B expression level, which resulted in the increase of Wee1 as well as Thr14/Tyr15 phosphorylated Cdk1 level. These changes resulted in decrease of Thr161 phosphorylated Cdk1 as well as cyclin B1 levels leading to MPF destabilization. The MPF destabilization leads to meiotic exit from diplotene arrest in several mammalian species (B).

Thr161 phosphorylated Cdk1 and cyclin B1 levels decreased significantly without altering the total Cdk1 level. These results suggest that the increased phosphorylation of Thr14/Tyr15 and decreased phosphorylation of Thr161 as well as cyclin B1 degradation destabilize MPF. The MPF destabilization mediates spontaneous as well as hCG-induced EDA in rat COCs cultured in vitro. Similarly, changes in specific phosphorylation status of Cdk1 have been reported during EDA in rat [10, 13, 14] and mouse [49, 50].

In conclusion, our results suggest that a moderate increase of ROS and decrease of cyclic nucleotide level mediate spontaneous as well as hCG-induced EDA during the achievement of meiotic competency in rat oocytes. The reduced cyclic nucleotide level decreased Cdc25B expression level, which resulted in the increase of Wee1 as well as Thr14/Tyr15 phosphorylated Cdk1 level. These changes resulted in decreased Thr161 phosphorylated Cdk1 as well as cyclin B1 levels leading to MPF destabilization. The MPF destabilization resulted in spontaneous EDA, progression via M-I to M-II stage to achieve the meiotic competency in rat oocytes. Thus, a moderate increase of ROS in a physiological range induces cyclic nucleotide-mediated destabilization of MPF that finally facilitates achievement of meiotic competency in rat COCs (**Figure 11**).

ACKNOWLEDGMENTS

This study was financially supported by Department of Science and Technology, Ministry of Science and Technology, Government of India (Grant No. EMR/2014/000702). The authors declare no conflicts of interest.

REFERENCES

1. Sirard MA, Desrosier S, Assidi M. In vivo and in vitro effects of FSH on oocyte maturation and developmental competence. *Theriogenology* 2007; 68 Suppl 1:S71–6. doi: 10.1016/j.theriogenology.2007.05.053.
2. Tripathi A, Kumar KV, Chaube SK. Meiotic cell cycle arrest in mammalian oocytes. *J Cell Physiol* 2010; 223(3):592–600. doi: 10.1002/jcp.22108.
3. Chaube SK, Prasad S, Tiwari M, Gupta A. Rat: an interesting model to study oocyte meiosis in mammals. *RRJZS* 2016; 4(3):25–7.
4. Chen ZQ, Ming TX, Nielsen HI. Maturation arrest of human oocytes at germinal vesicle stage. *J Hum Reprod Sci* 2010; 3(3):153–7. doi: 10.4103/0974-1208.74161.
5. Pandey AN, Tripathi A, Premkumar KV, Shrivastav TG, Chaube SK. Reactive oxygen and nitrogen species during meiotic resumption from diplotene arrest in mammalian oocytes. *J Cell Biochem* 2010; 111(3):521–8. doi: 10.1002/jcb.22736.
6. Tiwari M, Prasad S, Tripathi A, Pandey AN, Ali I, Singh AK, et al. Apoptosis in mammalian oocytes: a review. *Apoptosis* 2015; 20(8):1019–25. doi: 10.1007/s10495-015-1136-y.
7. Tiwari M, Prasad S, Tripathi A, Pandey AN, Singh AK, Shrivastav TG, et al. Involvement of reactive oxygen species in meiotic cell cycle regulation and apoptosis in mammalian oocytes. *Reactive Oxygen Species* 2016; 1(2):110–6. doi: 10.20455/ros.2016.817.
8. Wang ZW, Zhang GL, Schatten H, Carroll J, Sun QY. Cytoplasmic determination of meiotic spindle size revealed by a unique inter-species germinal vesicle transfer model. *Sci Rep* 2016; 6:19827. doi: 10.1038/srep19827.
9. Gilchrist RB. Recent insights into oocyte-follicle cell interactions provide opportunities for the development of new approaches to in vitro maturation. *Reprod Fertil Dev* 2011; 23(1):23–31. doi: 10.1071/RD10225.
10. Tiwari M, Chaube SK. Moderate increase of reactive oxygen species triggers meiotic resumption in rat follicular oocytes. *J Obstet Gynaecol Res* 2016; 42(5):536–46. doi: 10.1111/jog.12938.
11. Zhang M, Ouyang H, Xia G. The signal pathway of gonadotrophins-induced mammalian oocyte meiotic resumption. *Mol Hum Reprod* 2009; 15(7):399–409. doi: 10.1093/molehr/gap031.
12. Albertini DF. A cell for every season: the ovarian granulosa cell. *J Assist Reprod Genet* 2011; 28(10):877–8. doi: 10.1007/s10815-011-9648-z.
13. Pandey AN, Chaube SK. A moderate increase of hydrogen peroxide level is beneficial for spontaneous resumption of meiosis from diplotene arrest in rat oocytes cultured in vitro. *Biores Open Access* 2014; 3(4):183–91. doi: 10.1089/biores.2014.0013.
14. Prasad S, Tiwari M, Tripathi A, Pandey AN, Chaube SK. Changes in signal molecules and maturation promoting factor levels associate with spontaneous resumption of meiosis in rat oocytes. *Cell Biol Int* 2015; 39(6):759–69. doi: 10.1002/cbin.10444.
15. Tiwari M, Prasad S, Pandey AN, Premkumar KV, Tripathi A, Gupta A, et al. Nitric oxide signaling during meiotic cell cycle regulation in mammalian oocytes. *Front Biosci* (Schol Ed) 2017; 9:307–18.
16. Tiwari M, Prasad S, Shrivastav TG, Chaube SK. Calcium signaling during meiotic cell cycle regulation and apoptosis in mammalian oocytes. *J Cell Physiol* 2017; 232(5):976–81. doi: 10.1002/jcp.25670.
17. Gupta A, Tiwari M, Prasad S, Chaube SK. Role of cyclic nucleotide phosphodiesterases during meiotic resumption from diplotene arrest in mammalian oocytes. *J Cell Biochem* 2017; 118(3):446–52. doi: 10.1002/jcb.25748.
18. Chang HM, Qiao J, Leung PC. Oocyte-somatic cell interactions in the human ovary-novel role of bone morphogenetic proteins and growth differentiation factors. *Hum Reprod Update* 2016; 23(1):1–18. doi: 10.1093/humupd/dmw039.
19. Mangia F, Epstein CJ. Biochemical studies of

growing mouse oocytes: preparation of oocytes and analysis of glucose-6-phosphate dehydrogenase and lactate dehydrogenase activities. *Dev Biol* 1975; 45(2):211–20.
20. Palmer T, Jackson JB. A rapid burst preceding the steady-state rate of H^+-transhydrogenase during illumination of chromatophores of Rhodobacter capsulatus: implications for the mechanism of interaction between protonmotive force and enzyme. *FEBS Lett* 1990; 277(1–2):45–8.
21. Mohapatra SK, Sandhu A, Neerukattu VS, Singh KP, Selokar NL, Singla SK, et al. Buffalo embryos produced by handmade cloning from oocytes selected using brilliant cresyl blue staining have better developmental competence and quality and are closer to embryos produced by in vitro fertilization in terms of their epigenetic status and gene expression pattern. *Cell Reprogram* 2015; 17(2):141–50. doi: 10.1089/cell.2014.0077.
22. Salimi M, Salehi M, Masteri Farahani R, Dehghani M, Abadi M, Novin MG, et al. The Effect of melatonin on maturation, glutathione level and expression of h mgb1 gene in brilliant cresyl blue (BCB) stained immature oocyte. *Cell J* 2014; 15(4):294–301.
23. Catala MG, Izquierdo D, Uzbekova S, Morato R, Roura M, Romaguera R, et al. Brilliant cresyl blue stain selects largest oocytes with highest mitochondrial activity, maturation-promoting factor activity and embryo developmental competence in prepubertal sheep. *Reproduction* 2011; 142(4):517–27. doi: 10.1530/REP-10-0528.
24. Rodriguez-Gonzalez E, Lopez-Bejar M, Velilla E, Paramio MT. Selection of prepubertal goat oocytes using the brilliant cresyl blue test. *Theriogenology* 2002; 57(5):1397–409.
25. Opiela J, Katska-Ksiazkiewicz L, Lipinski D, Slomski R, Bzowska M, Rynska B. Interactions among activity of glucose-6-phosphate dehydrogenase in immature oocytes, expression of apoptosis-related genes Bcl-2 and Bax, and developmental competence following IVP in cattle. *Theriogenology* 2008; 69(5):546–55. doi: 10.1016/j.theriogenology.2007.11.001.
26. Su J, Wang Y, Li R, Peng H, Hua S, Li Q, et al. Oocytes selected using BCB staining enhance nuclear reprogramming and the in vivo development of SCNT embryos in cattle. *PLoS One* 2012; 7(4):e36181. doi: 10.1371/journal.pone.0036181.
27. Fakruzzaman M, Bang JI, Lee KL, Kim SS, Ha AN, Ghanem N, et al. Mitochondrial content and gene expression profiles in oocyte-derived embryos of cattle selected on the basis of brilliant cresyl blue staining. *Anim Reprod Sc*i 2013; 142(1–2):19–27. doi: 10.1016/j.anireprosci.2013.08.012.
28. Mohammadi-Sangcheshmeh A, Veshkini A, Hajarizadeh A, Jamshidi-Adegani F, Zhandi M, Abazari-Kia AH, et al. Association of glucose-6-phosphate dehydrogenase activity with oocyte cytoplasmic lipid content, developmental competence, and expression of candidate genes in a sheep model. *J Assist Reprod Genet* 2014; 31(8):1089–98. doi: 10.1007/s10815-014-0264-6.
29. Azari-Dolatabad N, Rahmani HR, Hajian M, Ostadhosseini S, Hosseini SM, Nasr-Esfahani MH. Effects of cilostamide and/or forskolin on the meiotic resumption and development competence of growing ovine oocytes selected by brilliant cresyl blue staining. *Theriogenology* 2016; 85(8):1483–90. doi: 10.1016/j.theriogenology.2016.01.008.
30. Kubiak JZ, Ciemerych MA, Hupalowska A, Sikora-Polaczek M, Polanski Z. On the transition from the meiotic to mitotic cell cycle during early mouse development. *Int J Dev Biol* 2008; 52(2–3):201–17. doi: 10.1387/ijdb.072337jk.
31. Premkumar KV, Chaube SK. Nitric oxide signals postovulatory aging-induced abortive spontaneous egg activation in rats. *Redox Rep* 2015; 20(4):184–92. doi: 10.1179/1351000215Y.0000000003.
32. Premkumar KV, Chaube SK. Increased level of reactive oxygen species persuades postovulatory aging-mediated spontaneous egg activation in rat eggs cultured in vitro. *In Vitro Cell Dev Biol Anim* 2016; 52(5):576–88. doi: 10.1007/s11626-016-0007-3.
33. Prasad S, Tiwari M, Koch B, Chaube SK. Morphological, cellular and molecular changes during postovulatory egg aging in mammals. *J Biomed Sci* 2015; 22:36. doi: 10.1186/s12929-015-0143-1.
34. Prasad S, Tiwari M, Pandey AN, Shrivastav TG, Chaube SK. Impact of stress on oocyte quality

and reproductive outcome. *J Biomed Sci* 2016; 23:36. doi: 10.1186/s12929-016-0253-4.
35. Prasad S, Tiwari M, Chaube SK. Abortive Spontaneous egg activation: an emerging biological threat for the existence of mammals. *Cell Reprogram* 2017; 19(3):145–9. doi: 10.1089/cell.2016.0052.
36. Tiwari M, Tripathi A, Chaube SK. Presence of encircling granulosa cells protects against oxidative stress-induced apoptosis in rat eggs cultured in vitro. *Apoptosis* 2017; 22(1):98–107. doi: 10.1007/s10495-016-1324-4.
37. Theofanakis C, Drakakis P, Besharat A, Loutradis D. Human chorionic gonadotropin: the pregnancy hormone and more. *Int J Mol Sci* 2017; 18(5). doi: 10.3390/ijms18051059.
38. Agarwal A, Durairajanayagam D, du Plessis SS. Utility of antioxidants during assisted reproductive techniques: an evidence based review. *Reprod Biol Endocrinol* 2014; 12:112. doi: 10.1186/1477-7827-12-112.
39. Shkolnik K, Tadmor A, Ben-Dor S, Nevo N, Galiani D, Dekel N. Reactive oxygen species are indispensable in ovulation. *Proc Natl Acad Sci USA* 2011; 108(4):1462–7. doi: 10.1073/pnas.1017213108.
40. Combelles CM, Gupta S, Agarwal A. Could oxidative stress influence the in-vitro maturation of oocytes? *Reprod Biomed Online* 2009; 18(6):864–80.
41. Adhikari D, Liu K. The regulation of maturation promoting factor during prophase I arrest and meiotic entry in mammalian oocytes. *Mol Cell* Endocrinol 2014; 382(1):480–7. doi: 10.1016/j.mce.2013.07.027.
42. Madgwick S, Jones KT. How eggs arrest at metaphase II: MPF stabilisation plus APC/C inhibition equals cytostatic factor. *Cell Div* 2007; 2:4. doi: 10.1186/1747-1028-2-4.
43. Liu W, Xin Q, Wang X, Wang S, Wang H, Zhang W, et al. Estrogen receptors in granulosa cells govern meiotic resumption of pre-ovulatory oocytes in mammals. *Cell Death Dis* 2017; 8(3):e2662. doi: 10.1038/cddis.2017.82.
44. Nunes C, Silva JV, Silva V, Torgal I, Fardilha M. Signalling pathways involved in oocyte growth, acquisition of competence and activation. *Hum Fertil* (Camb) 2015; 18(2):149–55. doi: 10.3109/14647273.2015.1006692.
45. Khazaei M, Aghaz F. Reactive oxygen species generation and use of antioxidants during in vitro maturation of oocytes. *Int J Fertil Steril* 2017; 11(2):63–70. doi: 10.22074/ijfs.2017.4995.
46. Cheon YP, Kim SW, Kim SJ, Yeom YI, Cheong C, Ha KS. The role of RhoA in the germinal vesicle breakdown of mouse oocytes. *Biochem Biophys Res Commun* 2000; 273(3):997–1002. doi: 10.1006/bbrc.2000.3052.
47. Wang Y, Teng Z, Li G, Mu X, Wang Z, Feng L, et al. Cyclic AMP in oocytes controls meiotic prophase I and primordial folliculogenesis in the perinatal mouse ovary. *Development* 2015; 142(2):343–51. doi: 10.1242/dev.112755.
48. Egbert JR, Uliasz TF, Shuhaibar LC, Geerts A, Wunder F, Kleiman RJ, et al. luteinizing hormone causes phosphorylation and activation of the cGMP phosphodiesterase PDE5 in rat ovarian follicles, contributing, together with PDE1 activity, to the resumption of meiosis. *Biol Reprod* 2016; 94(5):110. doi: 10.1095/biolreprod.115.135897.
49. Solc P, Schultz RM, Motlik J. Prophase I arrest and progression to metaphase I in mouse oocytes: comparison of resumption of meiosis and recovery from G2-arrest in somatic cells. *Mol Hum Reprod* 2010; 16(9):654–64. doi: 10.1093/molehr/gaq034.
50. Adhikari D, Busayavalasa K, Zhang J, Hu M, Risal S, Bayazit MB, et al. Inhibitory phosphorylation of Cdk1 mediates prolonged prophase I arrest in female germ cells and is essential for female reproductive lifespan. *Cell Res* 2016; 26(11):1212–25. doi: 10.1038/cr.2016.119.